

Photovoltaic properties and photoconductivity in multilayer Ge/Si heterostructures with Ge nanoislands

S. V. Kondratenko · O. V. Vakulenko · Yu. N. Kozyrev ·
M. Yu. Rubezhanska · A. G. Naumovets · A. S. Nikolenko ·
V. S. Lysenko · V. V. Strelchuk · C. Teichert

Received: 18 October 2010 / Accepted: 4 April 2011 / Published online: 12 April 2011
© Springer Science+Business Media, LLC 2011

Abstract Interband optical transitions in multilayer heterostructures with SiGe nanoislands were investigated using photocurrent spectroscopy and photo-emf. The *n-p* heterostructures containing Ge nanoislands in the area of the potential barrier were prepared by molecular-beam epitaxy at the temperature about 500 °C. It was shown that electron transitions from the ground state of the valence band in a nanoislands to the conduction band of Si surrounding made the main contribution into the vertical photo-emf in the range 0.75–1.05 eV, which is below the interband absorption edge of Si. The lateral photoconductivity observed in the range 0.63–0.8 eV at 77 K can be attributed to indirect interband transitions from the ground state of a nanoisland to *L*-state of the conduction band of a nanoisland. Analysis of Raman scattering spectra revealed that the Ge composition *x* in a nanoisland is about 0.87, while elastic deformation value amounts to $\varepsilon_{xx} = -0.016$. The calculated energies of interband transitions from the

ground state of a nanoisland to the conduction band of Si surrounding (0.63 eV) and to *L*-state of the conduction band of a nanoisland (0.81 eV) fit the experimental data with a rather good accuracy.

Introduction

Low-dimensional Ge/Si heterostructures show unique optical and electrical properties due to discrete energy spectrum of hole states of the valence band of SiGe nanoisland. Optical properties of multilayer Ge/Si heterostructures with SiGe nanoislands were mainly investigated using such methods as photoluminescence [1], optical absorption [2], Raman scattering [3], and photoconductivity [4]. Intraband transitions between the localized states in nanoislands in the spectral range below the c-Ge absorption edge are used for constructing of photodetectors with quantum dots [5] and laser heterostructures. There is another type of optical transitions possible in the II type heterostructures: interband transitions between the valence band states of the quantum dots and conduction band states of Si surrounding. Such transitions can be used for broadening of the spectral range of photodetector sensitivity [6], efficiency increase of solar elements [7], as well as optical recording and information read-out in memory cells [8]. The key factor in understanding of photoelectrical and optical properties of Ge/Si low-dimensional heterostructures is an influence of real values of Ge quantum dot composition and elastic deformation on electron spectra of such a system and nonequilibrium carrier transport in it.

The spectra of lateral and vertical photoconductivity (photo-emf) in multilayer Ge quantum dot structures prepared by molecular-beam epitaxy were investigated in this paper. The photoconductivity spectrum shape was attributed

S. V. Kondratenko · O. V. Vakulenko
Physics Department, Kiev National Taras Shevchenko University, 2 Acad. Glushkov Ave, Kiev 03022, Ukraine

Yu. N. Kozyrev · M. Yu. Rubezhanska (✉)
O.O. Chuiko Institute of Surface Chemistry, 17 Generala Naumova Str, Kiev 03164, Ukraine
e-mail: mruby@ukr.net

A. G. Naumovets
Institute of Physics, 46 Prospect Nauki, Kiev 03028, Ukraine

A. S. Nikolenko · V. S. Lysenko · V. V. Strelchuk
Institute of Semiconductor Physics, 46 Prospect Nauki, Kiev 03028, Ukraine

C. Teichert
Institute of Physics, Montanuniversitaet Leoben, Franz Josef Str. 18, 8700 Leoben, Austria

to interband transitions of electrons between hole states of the quantum dot valence band and the conduction band of Si surrounding. The energy-band diagram of Ge/Si heterojunction was also calculated taking into account the real values of the quantum dot composition and elastic deformation obtained from Raman scattering spectra.

Experimental technique

Multilayer Ge/Si heterostructures were prepared by molecular-beam epitaxy on *p*-type Si (100) substrates, doped by B, with resistivity $7.5 \Omega\text{cm}$. First, Si buffer layer of the thickness about 100 nm with B doping (10^{18} cm^{-3}) was grown on the substrate. The same B doping concentration was in the substrate. Then SiGe nanoisland layers were grown at temperature 500°C . The deposition rates were about 1.0 and 0.6 nm/min for Si and Ge, correspondingly. The Si spacer has been grown on SiGe nanoisland layers until the high resolution Si(100) 2×1 RHEED pattern was observed that is typical for the flat surface of Si. The period of the structure containing SiGe nanoisland layers and Si spacer was equal 5. The last SiGe nanoisland layer was covered with Si of the thickness 20 nm doped with Sb of the concentration 10^{18} cm^{-3} . Thus, *n-p* structures with SiGe nanoislands in the potential barrier area were grown. The scheme of such multilayer heterostructure is given in Fig. 1.

To investigate lateral photoconductivity of SiGe multilayer structures, two Au ohmic contacts with 1 mm in diameter and placed 5 mm apart were melted into the epitaxial layers at the temperature $T = 370^\circ\text{C}$ (Fig. 1a). The current–voltage dependencies of all the investigated structures were linear in the voltage range from $U = -50$ to $+50 \text{ V}$ at the temperatures range from 77 to 290 K.

Vertical photoconductivity and photo-emf spectra of barrier structures were investigated using a non-transparent Au contact from the Si substrate side and a half-transparent conducting Au contact of the thickness about 30 nm from the side of the upper layer Si (Fig. 1b). The current–voltage

dependencies of the vertical structures appeared to be rectified that can be explained by the presence of a potential barrier of *n-p* heterojunction.

Atomic force microscopy (AFM) measurements of control structure not covered by Si were carried out using NT-MDT Ntegra microscope and Si cantilevers with a tip radius $\sim 10 \text{ nm}$. It was found out that the average height of SiGe nanoislands was 2 nm, lateral size 24 nm, size dispersion $\sim 20\%$. The surface density of nanoislands was found to be 10^{10} cm^{-2} . Scarce dome islands with height about 12 nm, base diameter $\sim 70 \text{ nm}$, and surface density $\sim 10^8 \text{ cm}^{-2}$ are observed at once.

The photocurrent and photo-emf were measured in the range 0.6–2.0 eV using a standard lock-in amplification technique. The modulation frequency of the exciting irradiation was 30 Hz. The intrinsic spectral dependence of the experimental setup was eliminated by means of a pyroelectric optical detector.

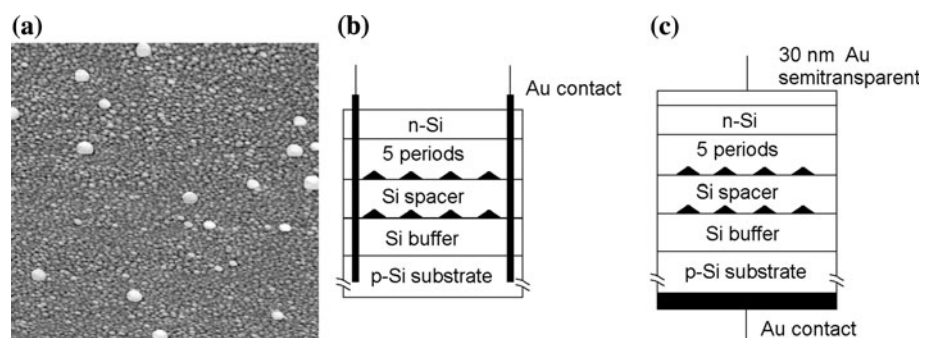
Micro Raman scattering spectra of the investigated structures were recorded at room temperature using automated Raman diffraction spectrometer T-64000 Horiba Jobin–Yvon equipped with CCD detector. The line 488 nm of Ar–Kr laser of 3 mW was used for excitation. Raman spectra were measured for the geometry $z(x,y) - x$, where axes x, y, z correspond to [100], [010], and [001] crystallographic directions, correspondingly. A long-focus lens Olympus, 50X, NA = 0 was used to focus the irradiation. Such geometry was chosen, since it is allowed for LO phonon scattering in Ge and Si and forbidden for two-phonon scattering of TA phonons in the Si substrate. This makes it possible to avoid difficulties in Raman spectra interpretation [9, 10].

Results and their discussion

Raman scattering

Composition and values of elastic strains in investigated Ge/Si heterostructures were estimated using Raman

Fig. 1 $3 \times 3 \mu\text{m}^2$ AFM image of Ge islands of uncaptured Si–Ge structures (a); Scheme of multilayer Ge/Si heterostructure for measurement of the lateral photoconductivity (b) and vertical photoconductivity and photo-emf (c)



spectroscopy. Typical Raman spectrum of Ge/Si heterostructure containing five layers of SiGe nanoislands is given in Fig. 2. It contains phonon bands corresponding to Ge–Ge, Si–Ge, and Si–Si vibrations, which is typical for SiGe heterostructures with nanoislands [11, 12]. Special feature of the observed Raman spectra is the doublet band behavior, that is particularly prominent for Ge–Ge and Si–Ge modes, which can be approximated by two Lorentz lines with maxima at 298.2 and 304.7 cm⁻¹ for Ge–Ge, as well as 404.4 and 419.5 cm⁻¹ for Si–Ge bands. This fact testifies the presence of two types of $\text{Si}_{1-x}\text{Ge}_x$ solid solutions with different composition and (or) elastic strains in studied structures. In case of SiGe heterostructures with nanoislands, this phenomenon can be generally attributed to nonuniform island structure [24] or their bimodal size and shape distributions [11–15]. Rather high growth temperature of the investigated structures (500 °C) allows excluding first possibility due to strong interdiffusion processes observed in such heterostructures [24]. Another possible reason of the doublet band behavior could be scattering in WL or Si/Ge interface, but the contribution of these regions to Raman spectra was shown to be negligible and reflects only in line broadening. From AFM measurements (Fig. 1a) investigated, nanoislands were shown to have bimodal size distribution with small hut-clusters (average height about 2 nm) and dome-shaped islands (average height about 20 nm). Taking this fact into account we consider observed doublet behavior of the phonon bands as related with contribution of different types of SiGe nanoislands.

For strained $\text{Si}_{1-x}\text{Ge}_x$, solid solution of nanoislands frequency positions of Si–Ge and Ge–Ge modes could be described as follows [11–15]:

$$\omega_{\text{Si-Ge}} = 400 + 29x - 95x^2 + 213x^3 - 170x^4 - b_s \epsilon_{xx}, \quad (1)$$

$$\omega_{\text{Ge-Ge}} = 282.5 + 16x - b_s \epsilon_{xx}, \quad (2)$$

where b_s is phonon deformation potential. It was shown recently [16] that the concentration dependence of the phonon deformation potential can be well approximated by the following relation:

$$b_s = b_4(x - 1)^4 + b_0, \quad (3)$$

where $b_4 = -190 \text{ cm}^{-1}$, b_0 amount to -460 and -555 cm^{-1} for Ge–Ge and Si–Ge phonon bands, correspondingly. Using frequency positions of Ge–Ge and Si–Ge phonon bands and relations (1–3), we determined composition and values of elastic strains for each type of $\text{Si}_{1-x}\text{Ge}_x$ nanoislands. Thus, Ge mole fraction and elastic strains in the small-sized nanoislands were found to be $x = 0.87$ and, $\epsilon_{xx} = -0.016$, correspondingly. For the dome-shaped nanoislands, these values were $x = 0.46$ and $\epsilon_{xx} = -0.023$.

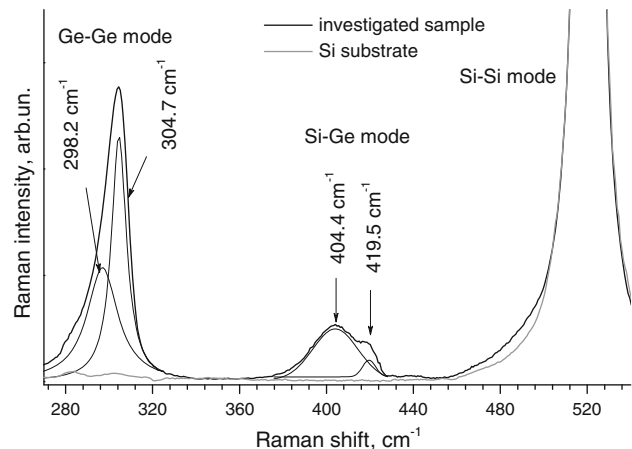


Fig. 2 Raman spectrum for 5-period Ge/Si heterostructure with SiGe nanoislands. The Raman spectrum for Si substrate of the investigated structure is given with a dashed line. The geometry of the experiment $z(x,y)-z$. $\lambda_{\text{exc.}} = 488.0 \text{ nm}$, $T = 300 \text{ K}$

Vertical photo-emf in multilayer Ge/Si heterostructures with Ge nanoislands

The spectral dependence of vertical photo-emf in multilayer Ge/Si heterostructure with SiGe nanoislands is given in Fig. 3. The minimal quanta energy, for which photo-emf generation was observed, amounted to 0.75 eV. The signal in the range 0.75–1.05 eV, where c-Si is transparent, is attributed to interband optical transitions involving the stated in the nanoislands (transition A in Fig. 6). The photo-emf signal was not observed for a similar structure without the quantum dots. The main contribution to vertical photo-emf and photocurrent signals with threshold energy of 0.75 eV gives carriers photoexcited in frequent nanoislands with 2 nm in height. Small contribution of scarce dome $\text{Si}_{0.54}\text{Ge}_{0.46}$ islands should be expected in the range $h\nu > 0.9 \text{ eV}$ [18].

Photo-emf generation in the considered structure can be attributed to separation of nonequilibrium electron–hole pairs by the electric field in the space charge area of $n-p$ heterojunction. The holes photogenerated in Si are shifted in the substrate direction, while electrons are shifted in the direction of the irradiated surface. These photoelectrons are free at interband transitions, while the holes are localized in the valence band of the nanoislands. The electron transport in the structure direction at the moment, when the holes are charged positively, creates a photo-emf signal with the same polarity as the electron–hole pairs generated in Si had.

The photoconductivity spectra at 290 and 77 K showed the same peculiarities, as the vertical photo-emf spectra had. The spectral dependence of vertical photo-emf in the structure Au/QDs/c-Si/Au at 77 K is given in Fig. 4.

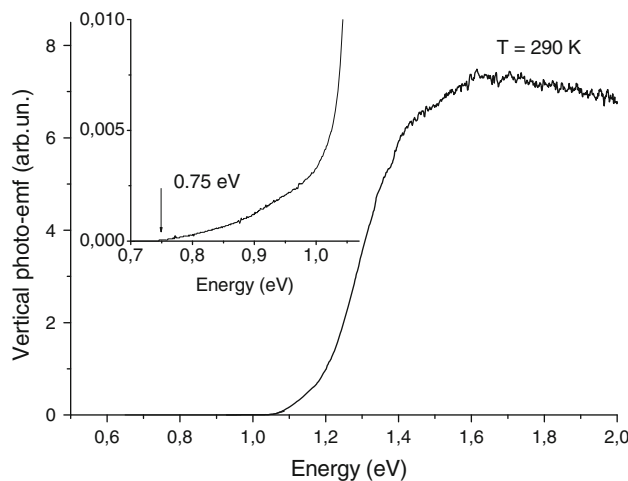


Fig. 3 Spectral dependence of the vertical photo-emf of Au/QDs-c-Si/Au structure at 290 K

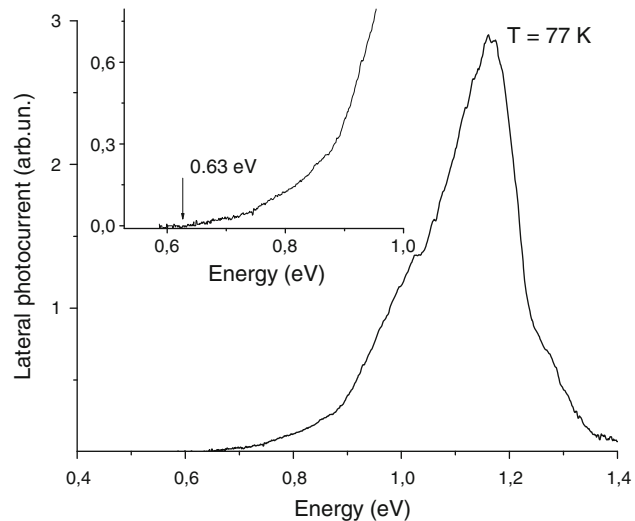


Fig. 5 Spectral dependence of the lateral photoconductivity for Ge/Si heterostructure, containing five layers of SiGe nanoislands

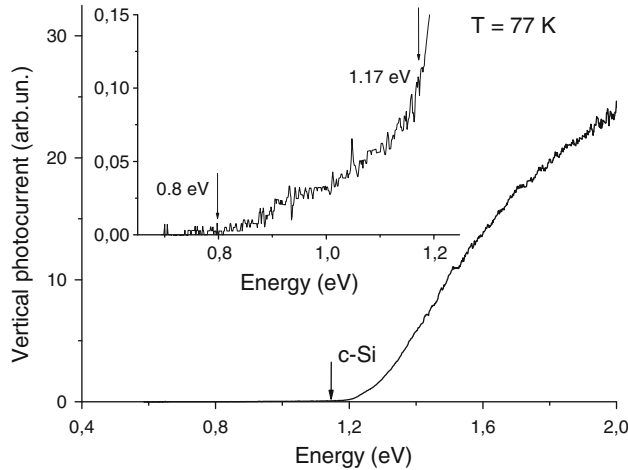


Fig. 4 Spectral dependence of the vertical photoconductivity for Au/QDs/c-Si/Au structure at 77 K

Interband transitions in the nanoislands give the photocurrent signal in the range 0.8–1.17 eV.

Lateral photoconductivity

A band bending of the conduction band exists in Si near the nanoislands, in which a spatial quantization level for electrons appears [17]. The influence of this level on optical and photoelectrical properties of *n-p* heterostructures with SiGe nanoislands was investigated in detail in the papers [18, 19]. Electron transitions from a conduction band level in Si surrounding to a valence band state in SiGe nanoislands contribute to the photoluminescence spectra in the range 0.6–0.9 eV depending on composition, size, and elastic deformation of the nanoclusters [20, 21]. The method of lateral photoconductivity made it possible

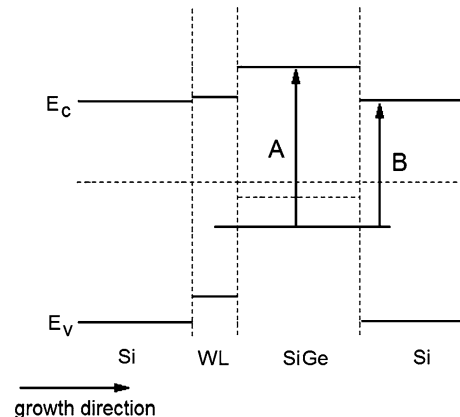


Fig. 6 Energy-band diagram of Ge/Si heterojunction with Ge nanoislands

to obtain detailed information about interband optical transitions in multilayer Ge/Si heterostructures with SiGe nanoislands. Earlier this method was applied for investigation of electron state spectra in similar heterostructures [22].

The electron–hole pairs generated by optical transitions between hole states in the nanoislands and the conduction band states in Si surrounding contribute to the lateral photoconductivity in the range 0.63–0.8 eV (Fig. 5). Interband transitions between the states in the valence and conduction bands of SiGe nanoislands become possible in the range $h\nu > 0.8$ eV. The observed transitions indirect in the space are marked with the arrow *B* in Fig. 6. The absence of their contribution to lateral photoconductivity and photo-emf spectra can be possibly explained by the presence of a potential barrier for electrons generated in Si surrounding of the nanoislands. The carriers generated in such a way have to overcome the barrier, whose height is

defined by the conduction band discontinuity of $\text{Si}_{1-x}\text{Ge}_x/\text{Si}$ heterojunction. That is why their contribution to the photocurrent signal and photo-emf is much smaller compared to the situation observed for the vertical photoconductivity, when nonequilibrium electron transport goes via intermediate Si layers and wetting layers. In this case a value of the conduction band discontinuity can be estimated as $0.8 - 0.63 = 0.17$ eV, that fits the calculation results given above.

Energy-band diagram and energies of optical transitions

Let us analyze the observed spectral dependences of photo-emf using the calculated energy-band diagram for Ge/Si heterostructures with SiGe nanoislands. The data on SiGe nanoisland composition and values elastic strains in them obtained from Raman spectra were used for calculation. It should be noted that the pressure values in the investigated SiGe/Si epitaxial heterostructures amount to several GPa leading to the electron spectrum shift for several hundreds meV.

The energies of interband transitions involving the nanoisland states depend on the values of the band discontinuities, composition and elastic strains, as well as an influence of the quantum confinement of carrier transport in the valence band of the nanoislands [23].

An average value of the valence band discontinuity $\Delta E_v^0 = 0.58 \cdot x$ [17] gives the best agreement between the theoretical and experimental data for relaxed $\text{Si}/\text{Si}_{1-x}\text{Ge}_x$ heterojunction.

Using the values of deformations (ε_{xx} , ε_{zz}) obtained from Raman spectra, one can estimate the value of the valence band discontinuity at the interfaces considering elastic deformations [18]:

$$\Delta E_v = \Delta E_v^0 + a_v \cdot (2 \cdot \varepsilon_{xx} + \varepsilon_{zz}) \quad (3)$$

where a_v is deformation potential for Ge. Thus, the value of valence band discontinuity of $\text{Si}_{1-x}\text{Ge}_x/\text{Si}$ heterojunction can be approximated by the dependence on mole fraction x in the following way: $\Delta E_v(x) = \Delta E_v^0 \cdot x$ [eV] [19].

The presence of biaxial strain in the nanoislands leads to degeneration lifting of the valence band, under which it is splitted and the heavy hole band shifts to lower energies with respect to the light hole band.

The shift values for light and heavy holes with respect to the average value ΔE_V can be determined taking into account the Raman scattering data for the investigated structures in the following way [24]:

$$\Delta E_{\text{LH}} = -\frac{1}{6} \Delta_0 + \frac{1}{4} \delta E + \frac{1}{2} \left[\Delta_0^2 + \Delta_0 \delta E + \frac{9}{4} (\delta E)^2 \right]^{1/2} \quad (4)$$

$$\Delta E_{\text{HH}} = -\frac{1}{3} \Delta_0 - \frac{1}{2} \delta E, \quad (5)$$

where the value δE in the case of deformation in [001] direction is $\delta E_{001} = 2a_v(\varepsilon_{zz} - \varepsilon_{xx})$. The values of spin-orbital splitting of the valence band Δ_0 , deformation potential a_v and elastic modules c_{12} , c_{11} for $\text{Si}_{1-x}\text{Ge}_x$ nanoislands are determined by a linear interpolation of the data for Si and Ge. As the calculations have shown, the values of the valence band discontinuities for heavy holes ΔE_{HH} and light holes ΔE_{LH} at 0 K amount to 0.65 and 0.55 eV, respectively.

To estimate the quantum confinement effect, let us consider a nanoisland as a three-dimensional rectangular potential well with walls of limit height. Doing so, the wall height will be defined by the calculated above band discontinuity values ΔE_{HH} and ΔE_{LH} for light and heavy hole subbands, correspondingly. As far as the heavy hole subband provides the dominant contribution ($\sim 85\%$) to hole states, let us restrict in the future by considering only the situation for the heavy hole subband. The effective mass of heavy holes m_{SiGe}^* was defined as $1/m_{\text{SiGe}}^* = x/m_{\text{Ge}}^* + (1-x)/m_{\text{Si}}^*$, where m_{Ge}^* , m_{Si}^* are the effective masses of heavy holes for pure germanium and silicon, that amount to $0.537m_0$ and $0.33m_0$, correspondingly. To estimate the allowed energy states, we have solved stationary Schrödinger equation for heavy holes in the potential well given in Fig. 6. Such a simplified model can be used only for rough estimation of the ground state in the nanoislands ($n = 1$). Wave functions and excitation energies depend on real shape and composition of the nanoislands much drastically leading to essential mistakes in energy transition estimation.

The calculated energy of the ground state (111) in the potential well of a nanoisland amounts to 0.12 eV. Correspondingly, the transition energy from the ground state of nanoisland to the conduction band of Si surrounding is 0.63 eV. According to our estimations, the threshold energy of interband transition from the ground state of a nanoisland to L state of the conduction band of a nanoisland amounts to 0.81 eV. Thus, a rather good agreement between the calculations and experimental values of interband transitions involving the ground state in a nanoisland were achieved.

Conclusion

Photocurrent and photo-emf signals in the infrared range, where c-Si is transparent, are caused by interband optical transitions via localized states of SiGe islands embedded into $n-p$ potential barrier of multilayer heterostructures. It

was shown that the electron transitions from the ground state of the valence band of a nanoisland to the conduction band of c-Si surrounding make the main contribution to the vertical photo-emf below the interband absorption edge of c-Si. The lateral photoconductivity observed in the range 0.63–0.8 eV at 77 K is caused by indirect in-space interband transitions from the ground state of a nanoisland valence band to *L*-state of nanoisland conduction band. Analysis of Raman scattering spectra revealed that the SiGe composition x in a nanoisland was about 0.87, while elastic deformation value amounted to $\varepsilon_{xx} = -0.016$. Scarce dome islands $\text{Si}_{0.54}\text{Ge}_{0.46}$ cause double-peak features corresponding to the Ge–Ge and Si–Ge Raman modes and give no effect on threshold values of photoconductivity and photo-emf spectra. The obtained data for x and ε were used for calculation of the energy-band diagram of Ge/Si heterojunction and hole state spectrum of nanoislands. The calculated threshold energies of interband transitions from ground state of nanoisland to conduction band of Si surrounding (0.63 eV) and to *L*-state of the nanoisland conduction band (0.81 eV) fit the experimental data with a rather good accuracy.

Acknowledgements The research was implemented within the bilateral ÖAD Project UA No 2009/08 and supported by the program of fundamental research of the National Academy of Sciences of Ukraine “Nanostructured systems, nanomaterials, nanotechnologies” through the Project No9/07 and by the Ministry of Education and Science of Ukraine through Project NoM/34-09.

References

1. Kamenev BV, Lee EK, Chang HY, Han H, Grebel H, Tsybeskov L, Kamins TI (2006) Appl Phys Lett 89:153106
2. Ramos LE, Furthmüller J, Bechstedt F (2005) Phys Rev B 72:045351
3. Gatskevich EI, Ivlev GD, Volodin VA, Dvurechenskii AV, Efremov MD, Nikiforov AI, Yakimov AI (2007) Proc SPIE 6728: 67281U
4. Lee SW, Park CJ, Kang TW, Cho HY, Hirakawa K (2005) Proc SPIE 5726:146
5. Colace L, Masini G, Assanto G, Luan HC, Kimerling LK (2006) ECS Trans 3:85
6. Yakimov AI, Dvurechenskii AV, Nikiforov AI, Proskuryakov YY (2001) J Appl Phys 89:5676
7. Alguno A, Usami N, Ujihara T, Fujiwara K, Sazaki G, Nakajima K, Shiraki Y (2003) Appl Phys Lett 83:1258
8. Bagraev NT, Bouravlev AD, Klyachkin LE, Malyarenko AM, Rykov SA (2001) Proc SPIE 4348:125
9. Kolobov AV (2000) J Appl Phys 87:2926
10. Baranov AV, Fedorov AV, Perova TS (2006) Phys Rev B 73:075322
11. Reparaz JS, Bernardi A, Goni AR, Alonso MI, Garriga M (2009) Phys Stat Sol B 56:1
12. Bernardi A, Alonso MI, Reparaz JS, Goni AR, Lacharmoise PD, Osso JO, Garriga M (2007) Nanotechnology 18:475401
13. Dvurechenskii AV, Smagina ZV, Zinoviev VA, Armbrister VA, Volodin VA, Efremov MD (2004) ZhETF Lett 79:411
14. Tan PH, Brunner K, Bougeard D, Abstreiter G (2003) Phys Rev B 68:125302
15. Alonso MI, de la Calle M, Osso JO (2005) J Appl Phys 98: 033530
16. Reparaz JS, Bernardi A, Goni AR (2008) Appl Phys Lett 92: 081909
17. Van de Walle CG (1989) Phys Rev B 39:1871
18. Kasper E (2000) Properties of silicon germanium and SiGe: carbon. INSPEC, London
19. Valakh MY, Yukhymchuk VO, Nikolenko AS (2007) Semicond Sci Technol 22:326
20. Kondratenko SV, Vakulenko OV, Kozyrev YN, Rubezhanska MY, Nikolenko AS, Golovinskiy SL (2007) Surf Sci 601:L45
21. Kondratenko SV, Vakulenko OV, Kozyrev YN, Rubezhanska MY, Nikolenko AS, Golovinskiy SL (2007) Nanotechnology 18: 185401
22. Talochkin AB, Chistokhin IB, Markov VA (2009) Nanotechnology 20:175401
23. Kozyrev YN, Kondratenko SV, Rubezhanska MY, Lysenko VS, Teichert C, Hofer C (2010) In: Shpak AP, Gorbyk PP (eds) Nanomaterials and supramolecular structures-physics chemistry and applications. Springer, Berlin, p 235. ISBN 978-90-481-2308-7
24. Valakh MY, Yukhymchuk V, Dzhagan VM, Lytvyn OS, Milekhin AG, Nikiforov AI, Pchelyakov OP, Alsina F, Pascual J (2005) Nanotechnology 16:1464